Aspects of Aqueous Iron and Manganese (II/III) Self-Exchange Electron Transfer Reactions

Kevin M. Rosso,*,† Dayle M. A. Smith,‡ and Michel Dupuis†

Pacific Northwest National Laboratory, P.O. Box 999, K8-96, Richland, Washington 99352, and Department of Physics, Whitman College, 345 Boyer Avenue, Walla Walla, Washington 99362

Received: November 13, 2003; In Final Form: March 23, 2004

Ab initio methods were applied to the calculation of the reorganization energy λ and the electronic coupling matrix element V_{AB} for the outer-sphere $Fe(OH_2)_6^{II/III}$ and $Mn(OH_2)_6^{II/III}$ self-exchange electron transfer (ET) reactions. For the Fe case, we find an appreciable effect on V_{AB} depending on whether the minority spin electron occupies the d_{xy} orbital or a mixture of d_{xz}/d_{yz} orbitals in the Fe^{II} ion. While these two possible nearly isoenergetic electron accepting states alter the magnitude and distance dependence of V_{AB}, they do not affect the internal reorganization energy λ_I to any significant level. The magnitude and distance dependence of V_{AB} are found to be strongly dependent on encounter orientation, as expected. V_{AB} values for corner-to-corner encounter orientations are substantially larger at any given ET distance considered than those for face-to-face encounter orientations. Values of the decay parameter β are in good agreement with well-accepted values. The adiabaticity criterion is tied to orientation and distance dependence of V_{AB}.

Introduction

Self-exchange electron transfer (ET) reactions of the type $M^X + M^{X+1} \rightarrow M^{X+1} + M^X$, where $M^{X/X+1}$ is a transition metal complex in aqueous solution undergoing a II/III oxidation-state change, historically have been a kind of test bench for scrutinizing molecular-scale processes controlling ET and theories that describe it.[1−3] The reaction involves three general steps: (1) diffusion of an M^{II} and an M^{III} ion together to form a precursor complex consisting of the solute and surrounding solvent, (2) transfer of an electron from M^{II} to M^{III} to form the successor complex, and (3) dissociation of the complex into separated products. Because the products of such a reaction are equivalent to the reactants and because no net energy change occurs, analysis of self-exchange reactions can yield information important for characterizing the intrinsic ET propensity of metal complexes.

For self-exchange ET reactions, the rate of ET in the precursor complex is strongly influenced by its structure. The connectivity of the reactants (inner vs outer sphere), the distance between them, their relative orientations, and the nature of the donor−acceptor orbitals all influence the ET rate. An important aspect of ET theory is its ability to capture these properties collectively within a small set of parameters. Taking the usual two-state approximation, we can discuss the ET reaction in terms of an initial state $\psi_A = M_1^{II}M_2^{III}$ before ET and final state $\psi_B = M_1^{III}M_2^{II}$ having energies that are parabolic with respect to nuclear coordinates. (The short-hand notation is used to indicate that complex M_1 is in oxidation state II or III and that complex M_2 in oxidation state III or II, respectively, in ψ_A and ψ_B, respectively. The wave functions actually computed do reflect such a characterization.) The reorganization energy λ is, in part, the energy to distort the precursor complex from its equilibrium structure for the reactants into the configuration of the products, or vice versa, without moving the electron. Electronic interactions between ψ_A and ψ_B are compactly described by the electronic coupling matrix element V_{AB}. Prediction of ET rates requires estimates for these two quantities, which together capture much of the configurational and electronic structure aspects of the precursor complex.[1]

However, precursor complex structures for reactions in solution are often not well known. The $Fe(OH_2)_6^{II/III}$ self-exchange ET reaction has been intensively studied from both experimental and theoretical perspectives,[4−12] but disagreement persists regarding the dominant pathway (inner vs outer sphere), owing in part to the complication of pH effects. Swaddle and co-workers[10] proposed parallel inner-sphere and outer-sphere pathways. Rustad and co-workers[7] pointed out the importance of $H_3O_2^-$ bridges in a precursor complex structure that falls between traditional inner and outer sphere. Most studies agree on the absence of a covalent bridge linking the $Fe^{II}-Fe^{III}$ pair in at least one component pathway of the overall ET reaction, which leads to weaker electronic coupling. This led Logan and Newton[4] to evaluate V_{AB} for different hypothetical outer-sphere precursor complex structures. The $Mn(OH_2)_6^{II/III}$ self-exchange ET reaction is viewed to follow an inner-sphere pathway exclusively, but the structure of a predominant precursor complex has not been identified.[13,14]

In this study, we calculate reorganization energies and electronic coupling matrix elements for the $Fe(OH_2)_6^{II/III}$ and $Mn(OH_2)_6^{II/III}$ self-exchange ET reactions. As discussed below, the former involves ET orbitals of $A_g(d_{xy})$ or $B_g(d_{xz}/d_{yz})$ symmetry depending on which d atomic-like orbital is occupied in the reduced complex, and the latter involves an ET orbital of A_g symmetry. In the absence of proven precursor complex structures, we chose hypothetical outer-sphere configurations following the approach of Logan and Newton.[4] We use ab initio calculations to evaluate the internal component of λ and V_{AB}, and we compare these with previous values where available. To the best of our knowledge, this is the first evaluation of V_{AB} for the outer-sphere Mn case using ab initio methods. Although the Mn self-exchange is likely inner sphere, evaluation of the outer-sphere case for comparison with Fe is instructive for

* To whom correspondence may be addressed. E-mail: kevin.rosso@pnl.gov. Tel.: (509) 376-7762. Fax: (509) 376-3650.
† Pacific Northwest National Laboratory.
‡ Whitman College.

10.1021/jp037470a CCC: $27.50
Published on Web 05/19/2004

understanding the dependence of V_{AB} on the reactant orientations, the donor−acceptor orbital, and the ET distance. Finally, we point out that the ab initio calculation of V_{AB} for the outer-sphere Fe self-exchange system has been studied extensively by Newton and co-workers.[4] We revisit this topic here partly to help clarify issues pertaining to the orbital occupation dependence of V_{AB}.

Theoretical Methods

Electron-Transfer Model. For the electron to move from M^{II} to M^{III} in the precursor complex, nuclear coordinates must first assume a configuration that brings the electronic energy levels of both ions into coincidence, whereupon the ET reaction is instantaneous with respect to nuclear motion.[15,16] The energy for the precursor complex as a collective whole is usually discussed in terms of two diabatic states as a function of nuclear coordinates q. The initial state $\psi_A = M_1^{II}M_2^{III}$ (before ET) and final state $\psi_B = M_1^{III}M_2^{II}$ (after ET) may be defined having energies E_A and E_B. Associated with each state is a potential-energy surface that is usually well approximated as parabolic with respect to q for small displacements in q.[17] Because self-exchange ET reactions yield products that are equivalent to the reactants, the potential energies of ψ_A in equilibrium configuration q_A and ψ_B in equilibrium configuration q_B are the same ($E_A = E_B$). From the same argument, it follows that the potential energy surfaces for ψ_A and ψ_B are symmetric with respect to each other and show a shape characteristic of a double well. Electron transfer is allowed to occur when the system has been excited to the configuration where ψ_A and ψ_B cross, the so-called crossing-point configuration q_C. This transition state can be envisioned as corresponding to the point when the nuclear coordinates of the M^{II} and M^{III} ions in the precursor complex each have been distorted into identical intermediate configurations, in which M−O bond distances in the reduced and oxidized complexes to assume intermediate values.[18] The energy at q_C is the activation energy ΔG^*.

The reorganization energy λ is the energy to distort the precursor complex and surrounding solvent from q_A to q_B, or vice versa, without moving the electron. Usually, λ can be discussed in terms of two largely independent contributions from the internal (or inner-sphere or intramolecular) part λ_I involving the energy to distort bonds and the external (or outer-sphere or extramolecular) part λ_E involving the energy to modify the polarization of the surrounding solvent due to the redistribution of charge in the internal part.[17] The total reorganization energy λ is taken as the sum of λ_I and λ_E. For parabolic potential-energy surfaces and the self-exchange case, the activation energy is related in a simple way to λ by $\Delta G^* = \lambda/4$. [17]

At q_C, the ET probability P depends on the amount of electronic coupling between ψ_A and ψ_B, in this case arising from direct interaction of metal d orbitals or interaction through water ligands. The coupling is compactly described by the electronic coupling matrix element V_{AB}, which increases with increasing electronic interaction between ψ_A and ψ_B at q_C. If the interaction is weak, upon excitation to q_C, the system will predominantly remain on the ψ_A surface and will rarely crossover onto the ψ_B surface. If the interaction is strong, two new adiabatic states are formed from the diabatic ones. In this case, the system evolves on the new lower surface and, barring multiple crossings, excitation to q_C results in the ET products being formed. The weak interaction case is conventionally referred to as the nonadiabatic case (or diabatic), and the strong interaction case is referred to as adiabatic.

If the ET is nonadiabatic, as many involving $Fe^{II/III}$ and $Mn^{II/III}$ self-exchange are, only a fraction of the system passes through q_C on the ψ_A surface ends up on the ψ_B surface.[2] This observation allows the ET rate to be calculated using expressions based on Fermi's golden rule, which implicitly assumes nonadiabaticity.[1] However, because here we are re-evaluating the distance and orientation dependence of V_{AB}, with very little extra effort, we can also assess the distance dependence of P. Thus, we can estimate the distance cutoffs at which these ET reactions switch between adiabatic and nonadiabatic behavior. In anticipation of having to treat both adiabatic and nonadiabatic cases, it was convenient to compute P using the semiclassical expression obtained from Landau and Zener[19−21] which gives

$$P = 1 - \exp(-2\pi\gamma) \tag{1}$$

where

$$\gamma = 2\pi V_{AB}^2/[h\nu|S_A - S_B|] \tag{2}$$

and S_A and S_B are the slopes of the potential energy surfaces for ψ_A and ψ_B, and ν is the velocity of the system through q_C (assumed constant). We take $\nu = (2kT/\pi m)^{1/2}$, where m is the reduced mass.[22] The Landau−Zener expression describes the ET probability for a single passage through q_C. For descriptive purposes, we may consider the principal single passage event to be a thermal excitation upward in energy through q_C. The overall reaction probability must be based on the additional consideration of multiple passages through q_C, which includes, for example, the descent of the system back down through q_C where a finite probability of a hop from one surface to another also exists. The overall reaction probability is referred to as κ and, for self-exchange systems, is related to P by[2]

$$\kappa = \frac{2P}{1+P} \tag{3}$$

This overall probability κ is also known as the transmission coefficient and is used as the pre-exponential electronic factor term in Marcus' famous ET rate equation based on Eyring's transition state theory.[17] Methodological details pertaining to the calculation of V_{AB}, λ, and the potential energy surfaces using ab initio calculations are described below.

Ab Initio Calculations. All ab initio calculations were performed using NWChem.[23] For the calculations pertaining to the structure of an outer-sphere precursor complex, the four ion species $Fe(OH_2)_6^{2+}$, $Fe(OH_2)_6^{3+}$, $Mn(OH_2)_6^{2+}$, and $Mn(OH_2)_6^{3+}$ were separately optimized. We carried out these geometry optimizations using the open-shell B3LYP hybrid functional,[24,25] which has performed well for similar transition metal ions in the past.[26−31] Basis sets used were the Ahlrich valence triple-ζ basis set for iron and manganese[32] and 6-311++G** for the oxygen and hydrogen atoms.[33−35] Starting guesses for the open-shell density of each ion cluster were calculated from wave functions for the separated metal cations and water fragments. All four ion clusters were treated as high spin using the open-shell density functional theory (DFT) method, with a concatenated fragment orbital guess (with water and metal ion fragments) in order to establish 3d orbital occupation numbers with the desired spin structure. No symmetry restrictions were imposed on the geometry optimizations. Nuclear coordinates and total energies resulting from these calculations were used in the calculation of V_{AB} and λ_I, respectively, for the outer-sphere precursor complexes. Note, as described below, by

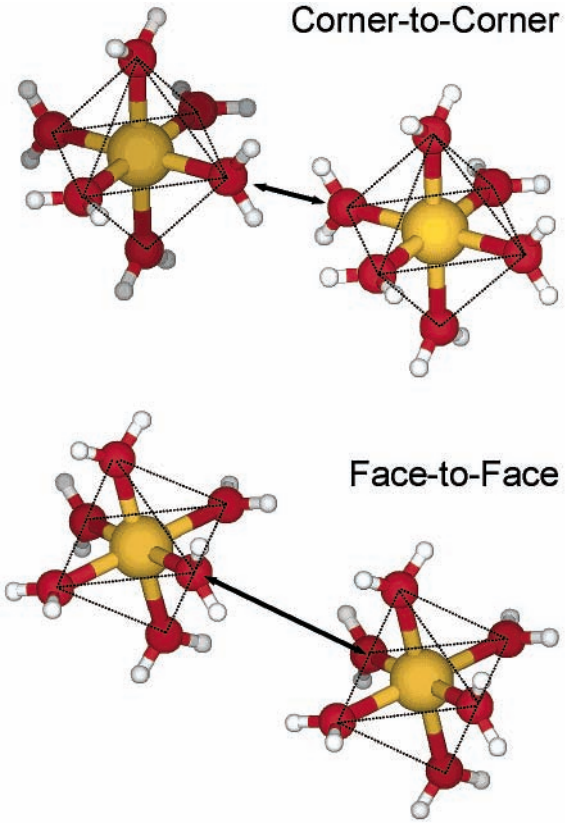

Figure 1. Ball-and-stick models of the corner-to-corner and staggered face-to-face outer-sphere precursor complex configurations.

necessity due to current formalism restriction, the V_{AB} calculations for the outer-sphere complexes were performed using UHF wave functions with structures optimized with the B3LYP method.

Electronic Coupling. The calculation of V_{AB} was performed for the precursor complexes at predicted crossing-point configurations. To determine the configuration at q_C, we used the linearized reaction coordinate approximation. When the potential-energy surfaces are parabolic, a good approximation of the reaction coordinate is given by[36]

$$q(\xi) = \xi q_A + (1 - \xi) q_B \tag{4}$$

By use of $1 \geq \xi \geq 0$, q can smoothly change from q_A ($\xi = 1$) to q_B ($\xi = 0$) going through q_C ($\xi = {}^1/_2$). Outer-sphere precursor complexes were constructed by computing the coordinates for the $\xi = {}^1/_2$ transition state from the separately optimized monomer structures. The transition state structure was then duplicated in space, and the ions were rotated to achieve the desired orientation. Two encounter orientations were chosen, corner-to-corner- and face-to-face-oriented octahedra (Figure 1), for comparison with the similar choices made by Newton and co-workers.[4−6] The corner-to-corner orientation involves aligning a pair of M−OH_2···H_2O−M bonds, one from each reactant (Figure 1a). The face-to-face orientation involves aligning the reactants along the (quasi) C_3 symmetry axes, with a relative rotation of one of the reactants by 60° so as to stagger the ligands (Figure 1b). For the face-to-face orientation, molecular orbitals were rotated while maintaining orbital symmetry on the separate monomers so as to allow for maximum overlap. The ET module in NWChem uses the method of corresponding orbital transformation to bi-orthogonalize the overlap between the spin orbitals of the ET states ψ_A and ψ_B, thereby simplifying the evaluation of the Hamiltonian between them using Slater's rules.[37]

The electronic coupling matrix element V_{AB} at q_C is given by[36]

$$V_{AB} = \frac{|H_{AB} - S_{AB}(H_{AA} + H_{BB})/2|}{1 - {S_{AB}}^2} \tag{5}$$

where $H_{ij} = \langle \psi_i | H | \psi_j \rangle$ and i and j are equal to A or B, $S_{AB} = \langle \psi_A | \psi_B \rangle$, and H is the exact total electronic Hamiltonian. Calculations of V_{AB} were performed using NWChem[23] using UHF wave functions. Basis sets used were as described above, except the metal atom basis sets were augmented with diffuse functions to improve the description of the participating metal orbitals in electronic coupling. Specifically, the Fe basis set was augmented with (function/exponent) s/0.01257, p/0.04184, and d/0.11330.[38] The Mn basis set was augmented with s/0.01189, p/0.04028, and d/0.10540.[38]

Reorganization Energy. The internal component of the reorganization energy λ_I was defined to consist of the clusters themselves, and the hypothetical surrounding solvent water was treated as the external part. Computing the internal reorganization energy λ_I generally involves evaluating the energy to distort the nuclear configuration while maintaining a particular electronic structure. Two methods to compute λ_I using ab initio calculations were discussed previously, which are the "direct"[18] and "4-point"[39] methods. The former method involves calculating the distortion energy for the supermolecular cluster (containing both ET reactants) and is best for cases when the ET reactants are covalently coupled, i.e., through a bridging group. The 4-point method involves treating reactants as infinitely separated fragments and computing λ_I from the distortion energies for the separate reactants; four ab initio total energies are required. It assumes the ET reactants are independent of each other, and it is often simpler to execute. This method has been successfully applied to ET systems where the reactants are structurally distinct units or are connected by a long molecular bridge.[18,26,31,40−42] We used the 4-point method in this study.

To evaluate the slopes of the potential energy surfaces q_C, as described below, we need an estimate of the external reorganization energy to add to λ_I. λ_E usually makes a large contribution to the total reorganization energy for the systems in question here because of the small cavity sizes.[3,26,43] Here we estimated λ_E using the continuum equation of Marcus,[17] which gives

$$\lambda_E = (\Delta e)^2 \left(\frac{1}{2r_1} + \frac{1}{2r_2} - \frac{1}{r}\right)\left(\frac{1}{D_{op}} - \frac{1}{D_s}\right) \tag{6}$$

where Δe is the charge transferred, r_1 and r_2 are radii for the donor and acceptor cavities in the continuum model, r is the ET distance, and D_{op} and D_s are the optical and static dielectric constants of water, respectively. Cavity radii were taken as the average M−O bond distances calculated for the ab initio clusters described above.[26] We used $D_{op} = 1.77$ and $D_s = 78.39$.

Potential-Energy Surfaces. To evaluate the Landau−Zener probabilities, the slopes S_A and S_B of the potential energy surfaces at the crossing-point configurations are needed in units of energy/distance. Configurational changes in high-spin Fe and Mn hexaqua complexes due to II/III valence change primarily involve Fe−O and Mn−O bond-length modification. Therefore, for both Fe and Mn separately, we used the average of the calculated M−O distances associated with the II/III valence change as a distance proxy value for the linearized reaction coordinate parameter ζ. Hence, assuming that the potential-

TABLE 1: M−O Bond Lengths (Å) in $M(OH_2)_6$ Monomer Clusters Calculated Using B3LYP and Comparison with Values Determined by EXAFS Measurements of the Aqueous Ions

M−O bond	Mn^{III}	Mn^{II} A_g	Fe^{III}	Fe^{II} $A_g(d_{xy})$	Fe^{II} $B_g(d_{xz},d_{yz})$
1	1.949	2.218	2.059	2.136	2.142
2	1.949	2.218	2.059	2.137	2.143
3	2.094	2.218	2.059	2.218	2.160
4	2.094	2.218	2.059	2.219	2.161
5	2.098	2.218	2.059	2.140	2.186
6	2.098	2.218	2.059	2.143	2.186
exp[45]		2.177	1.990	2.095	2.095

energy surfaces are parabolic, the only other requirement to enable evaluation of S_A and S_B at q_C was knowledge of the activation energy ΔG^*. The activation energy was estimated using $\Delta G^* = (\lambda_I + \lambda_E)/4$, with λ_I computed from the total energy method described above and λ_E computed using Marcus' continuum equation, also as described above. Previous work on related systems suggests that the parabolic approximation is a good one.[18]

Results and Discussion

Monomer Structures and Reorganization Energies. The II/III valence interchange for high-spin $Fe(OH_2)_6$ involves the transfer of the minority spin electron occupying the t_{2g} subset of the Fe(3d) orbitals (dπ-type ET). For the Fe^{III} hexaqua ion, five 3d majority spin electrons are distributed uniformly among the five 3d orbitals (d_{z^2}, $d_{x^2-y^2}$, d_{xy}, d_{xz}, d_{yz}). Consequently, the structure resulting from geometry optimization (symmetry unconstrained) using B3LYP is highly symmetric (T_h point-group symmetry) with all six Fe−O distances at 2.059 Å (Table 1).

For the Fe^{II} hexaqua ion, the minority spin electron occupying the t_{2g} orbitals causes a Jahn−Teller distortion in the structure that breaks the symmetry. With respect to Fe−O bond lengths, this distortion is well known. It involves the differentiation of Fe−O bond lengths into three sets of pairs, with equivalent bonds diametrically opposed from each other about the Fe atom. Another aspect of the distortion involves the rotation of the H_2O ligands about the Fe−O bond axes. This kind of rotation has been predicted for other metal hexaqua ions possessing a nonuniform occupation of the t_{2g} 3d orbitals.[44] This aspect of the Fe^{II} hexaqua ion structure is overlooked often in ab initio structure optimizations because a variety of geometric symmetry constraints are usually imposed. Here we have used no geometric symmetry constraints (i.e., the C1 point group). Collectively, the distortion reduces the symmetry from T_h to C_{2h}.

Analysis of the character table for the C_{2h} point group yields two possible electron accepting states, with symmetry labels A_g and B_g, based on whether the minority spin electron occupies the d_{xy} orbital or a mixture of the d_{xz}/d_{yz} orbitals, respectively. The optimized bond lengths for the Fe^{II} hexaqua ion in the A_g-(d_{xy}) and $B_g(d_{xz},d_{yz})$ states are given in Table 1. The energies calculated for these structures are similar, with the $B_g(d_{xz},d_{yz})$ state lower in energy than the $A_g(d_{xy})$ state by only 4.5×10^{-4} Hartrees (0.3 kcal/mol), suggesting that both states are equally likely.

The Mn^{II} hexaqua ion shares the symmetric d^5 high-spin arrangement that is found in the Fe^{III} hexaqua ion. The calculated optimal Mn^{II}−O bond length is 2.218 Å, with all six bonds equivalent and with T_h point-group symmetry found for the whole cluster (Table 1). The $Mn^{II/III}$ valence interchange involves the transfer of one of the majority spin electrons occupying the e_g subset of the Mn(3d) orbitals. Optimizations (symmetry unconstrained) of the Mn^{III} hexaqua ion yield a distorted structure involving a pairwise differentiation of Mn−O bonds as described above but with no H_2O rotation (the t_{2g} orbitals in this case are uniformly occupied) and D_{2h} point-group symmetry. Analysis of the character table for the D_{2h} point group indicates that removal of an electron from either the d_{z^2} or $d_{x^2-y^2}$ orbitals of Mn^{II} yields the same irreducible representation A_g. The optimized bond lengths calculated for Mn^{II} and Mn^{III} hexaqua ions are given in Table 1. Calculated bond lengths for both the Fe and Mn ions are on average 3% greater than from measurements of the aqueous ions using the extended X-ray absorption fine structure method (EXAFS).[45] Accuracy problems for transition metal M−O bond lengths using B3LYP have been previously documented.[46,47] However, the average calculated bond length changes associated with the III → II oxidation state change are essentially identical to the 0.11 Å (Fe)[45] and 0.17 Å (Mn)[3] experimental values.

The internal components of the reorganization energy λ_I for $Fe^{II/III}$ and $Mn^{II/III}$ self-exchange ET demonstrate the high sensitivity of λ_I to the e_g vs t_{2g} nature of the ET orbital. Values for λ_I computed using the 4-point method[39] and comparisons with values reported elsewhere are given in Table 2. λ_I values analogous to experimental ones can be determined from[12]

$$\lambda_I = 3(f_{II} + f_{III})(d_{II} - d_{III})^2 \qquad (7)$$

where f_i is the breathing force constant for oxidation state i, for which $f_i = 4\pi\nu_i^2 c^2 \mu$, with ν_i as the measured breathing frequency and the reduced mass μ equal to the mass of one water molecule and d_i is a measured M−O bond distance at equilibrium. Values determined in this way are listed in Table 2 for comparison with the ab initio values.

In all cases, the internal reorganization energy for the $Mn^{II/III}$ self-exchange ET reaction is substantially higher than that for the $Fe^{II/III}$ self-exchange ET reaction because the ET orbital is part of the e_g subset of the Mn(3d) orbitals. The e_g orbitals are oriented along the Mn−O bonding directions and have strong σ-type interactions with ligand orbitals. Changing the occupation of the e_g orbitals has a large effect on the Mn−O interaction, producing large Mn−O bond-length changes and a large λ_I. The ET orbital for the $Fe^{II/III}$ self-exchange ET reaction involves the t_{2g} subset of Fe(3d) orbitals, which are oriented along the quasi-2-fold symmetry axes bisecting the octahedral edges. These orbitals do not interact strongly with ligand orbitals. Thus, changing the occupation of the Fe(3d) t_{2g} orbitals has less of an influence on Fe−O bond lengths, and λ_I for $Fe^{II/III}$ self-exchange ET is lower than for $Mn^{II/III}$ self-exchange ET. The calculations for the $Fe^{II/III}$ self-exchange ET also indicate that λ_I depends very little on whether the electron-accepting orbital is of $A_g(d_{xy})$ or $B_g(d_{xz},d_{yz})$ character (Table 2).

Values of λ_I estimated using eq 7 with experimental frequencies and bond lengths are markedly lower than values calculated using the 4-point method with ab initio energies (Table 2). Both methods treat the ions as infinitely separated fragments; hence, the difference does not arise from exclusion of possible effects from interdependence of the reactants. We attribute the differences between the ab initio values and the "experimental" ones in part to the fact that experimental normal mode frequencies other than M−O stretching frequencies are not readily available for these ions, especially the trivalent ones, and therefore the analysis using eq 7 misses possible contributions to λ_I from other reorganizing motions. One example is the rotation of ligands already mentioned for the Fe case.

TABLE 2: Internal Reorganization Energies λ_I (eV) Computed Using the 4-Point Method[39] and from "Experiment" for Outer-Sphere Self-Exchange ET Reactions[a]

	B3LYP/AhlrichsVTZ/6-311++G**/-gas-phase (this study)			B3LYP/6-311+G/-gas-phase (ref 26)	B3LYP/6-311+G/PCM (ref 31)	exp[b]
	λ_I^{II}	λ_I^{III}	λ_I	λ_I	λ_I	λ_I
Mn A_g	0.933	0.978	1.911	1.788	2.40	0.72[c]
Fe$A_g(d_{xy})$	0.321	0.365	0.686	0.611	0.82	0.31[d]
Fe$B_g(d_{xz},d_{yz})$	0.336	0.363	0.699			

[a] $\lambda_I = \lambda_I^{II} + \lambda_I^{III}$. [b] The "experimental" values are determined using Equation 7 and consider only the M−O breathing motions of the ions. The formulation requires breathing frequencies and the difference in equilibrium M−O bond lengths for the II and III ions, all of which we take from experiment. [c] Frequencies taken as 366 cm^{-1} for Mn^{II} [50] and 510 cm^{-1} for Mn^{III}.[51] The Mn−O bond length change is taken as 0.17 Å.[3] [d] Frequencies taken as 388 cm^{-1} for Fe^{II} and 506 cm^{-1} for Fe^{III}.[50] The Fe−O bond length change is taken as 0.11 Å.[45]

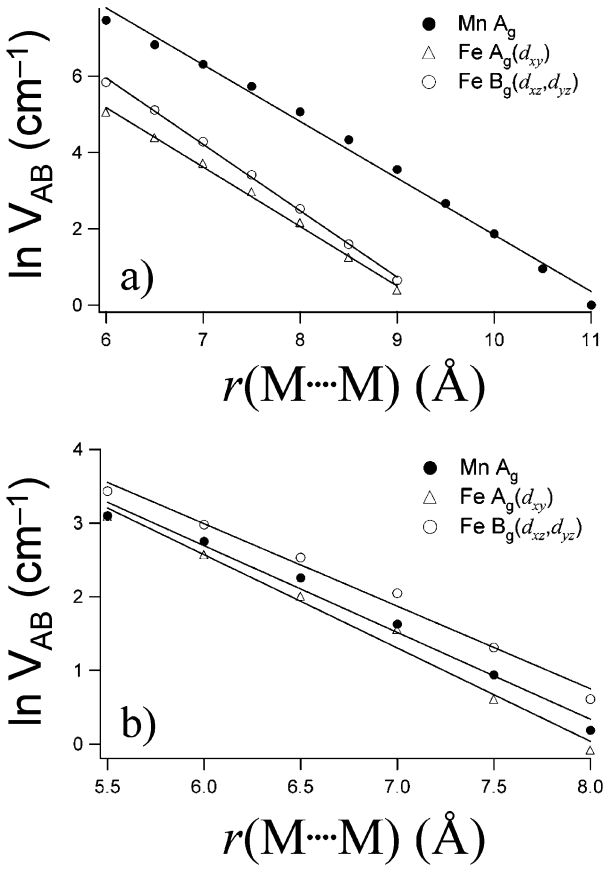

Figure 2. Calculated distance dependence of V_{AB} for the (a) corner-to-corner and (b) face-to-face precursor complexes.

Electronic Coupling. In turning our attention to the electronic coupling matrix element V_{AB} for the self-exchange ET reactions, the focus also shifts from equilibrium configurations of the reactants to the transition state configurations at the crossing point q_C. Values for V_{AB} at q_C calculated as a function of the metal−metal separation distance r for both the corner-to-corner and face-to-face encounter orientations for the reactants are shown in Figure 2. In general, the magnitude and distance dependence of V_{AB} are found to be strongly dependent on encounter orientation. The V_{AB} value for the corner-to-corner encounter orientation is substantially larger at any given distance considered than that for the face-to-face encounter orientation. We interpret this to mean that superexchange interaction mediated by the water ligands (in the first coordination shell) efficiently increases the electronic coupling relative to the direct "through-space" coupling, even for outer-sphere encounter complexes, consistent with previous work on this topic.[6] For the corner-to-corner encounter orientation, significant differences between Fe and Mn cases are apparent, with the Fe $A_g(d_{xy})$ and Fe $B_g(d_{xz},d_{yz})$ cases behaving similarly to each other (Figure 2a). For the face-to-face encounter orientation (Figure 2b), the magnitude and distance dependence of V_{AB} for all three self-exchange ET cases considered are rather similar [Mn A_g, Fe $A_g(d_{xy})$, Fe $B_g(d_{xz},d_{yz})$]. It is likely that at least part of the larger V_{AB} found for Mn relative to the Fe cases for the corner-to-corner orientation could be explained by larger superexchange interactions.

In all cases, an exponential decay in V_{AB} with increasing distance is predicted as expected.[2] The absolute value of the slope of linear fits to ln V_{AB} as a function of r equate with the decay parameter β, which is conventionally used in expressions of the type[2]

$$V_{AB} = V_{AB}^{0} \exp[-\beta(r - r_0)/2] \qquad (8)$$

where V_{AB}^0 is the value of V_{AB} at the optimal separation distance r_0. Values for β calculated in this study and comparisons with those reported elsewhere are given in Table 3. We note that values of β calculated here are for the gas phase and at larger separations would likely be affected by superexchange effects associated with the presence of intervening solvent molecules.[48] For the face-to-face encounter orientation, our values of β for Fe self-exchange ET (Fe $A_g(d_{xy}) = 2.5$ $Å^{-1}$, $B_g(d_{xz},d_{yz}) = 2.3$ $Å^{-1}$) compare well with the 2.4 $Å^{-1}$ value of Logan and Newton.[4] Also in Table 3, we give the remaining parameter ln $V_{AB}^{r=0}$ (cm^{-1}) that when combined with β gives the equations for the lines of the form ln V_{AB} (cm^{-1}) = ln $V_{AB}^{r=0}$ (cm^{-1}) − $\beta(r)/2$ fit to the points in Figure 2. We use these linear fits to interpolate values of V_{AB} for comparison with other electronic coupling terms at specific values of r. The optimal values of r (i.e., r_0) for transition metal hexaqua ion self-exchange ET are thought to be in the range 5−9 Å.[1−3] Newton and others have estimated $r_0 = 5.5$ Å for the Fe case.[2,8] To facilitate direct comparison between our values of V_{AB} with those calculated by Newton and co-workers, our values at 5.5 Å for the face-to-face orientation are given in Table 3.

Very little information is available on the electronic coupling and optimal values of r for Mn self-exchange ET. At least two studies have placed r at 5−7 Å for Mn self-exchange ET.[26,49] At $r_0 = 6.85$ Å, Bu and co-workers[49] compute a phenomenological electronic coupling term = 76.9 cm^{-1}, which can only be indirectly compared with our V_{AB} values of 678 cm^{-1} for corner-to-corner and 5 cm^{-1} for face-to-face orientations at that value of r. For the corner-to-corner orientation, Newton and co-workers selected 7.3 Å as a lower limit for accessible Fe−Fe distances.[4] We tabulate our calculated values of V_{AB} for $r =$ 7.3 Å for the corner-to-corner Fe and Mn cases for direct comparison. By this we do not imply that Fe and Mn should have similar optimal r values; differences in ionic radii would likely differentiate the two somewhat in terms of optimal r values.

TABLE 3: Calculated Values for β and V_{AB}

self-exchange ET reaction	β (Å^{-1})	ln $V_{AB}^{r=0}$ (cm^{-1})	r^a (Å)	V_{AB} (cm^{-1}) this study	V_{AB} (cm^{-1}) ref 4	V_{AB} (cm^{-1}) ref 5	V_{AB} (cm^{-1}) ref 6
			Corner-to-Corner				
Mn A_g	2.972	16.698	7.3	347			
$FeA_g(d_{xy})/B_g(d_{xz},d_{yz})$	3.116/3.480	14.527/16.391	7.3	23/40	27	12	25
			Face-to-Face				
Mn A_g	2.356	9.763	5.5	27			
$FeA_g(d_{xy})/B_g(d_{xz},d_{yz})$	2.534/2.242	10.171/9.715	5.5	25/35	98	50	49

[a] Values of r are taken from Logan and Newton computed for the Fe case.[4] The same values of r are applied here to Fe and Mn cases to facilitate direct comparison and do not imply similar optimal separation distances for Fe and Mn.

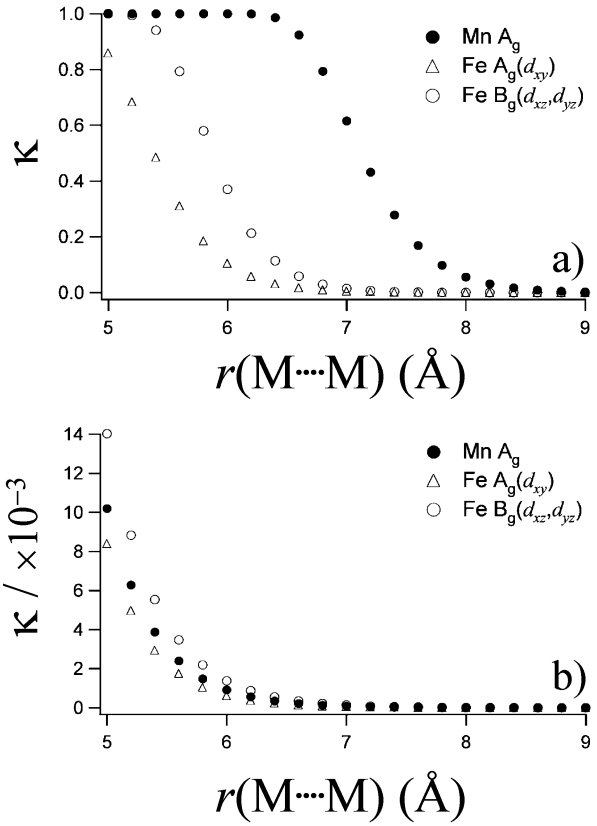

Figure 3. Calculated distance dependence of the transmission coefficient for the (a) corner-to-corner and (b) face-to-face precursor complexes.

Transmission Probabilities. The self-exchange ET reactions in this study have typically been classified as nonadiabatic (i.e., $\kappa < 1$).[2,3,49] Evaluation of the adiabaticity for the overall reactions usually requires prior knowledge of, among other things, r_0. The reason r_0 must be known is because of the distance dependence of both V_{AB} and λ_E. V_{AB} is an important term in the Landau−Zener model described above. Indirectly, λ_E is as well because it modifies the activation energy ΔG^* and therefore it modifies the slopes of the potential energy surfaces at q_C. Calculation of the optimal ET distances from first principles can be a difficult problem, likely involving orientational averaging of the encounter complex. Proceeding without exact knowledge of r_0, here we calculate the distance dependence of κ over the generally accepted 5−9 Å range of r (Figure 3).

Several conclusions may be obtained from the Landau−Zener calculations. Adiabatic behavior ($\kappa \approx 1$) is predicted for the corner-to-corner encounter orientation at the shorter end of the ET distance range. For this orientation, the transition from adiabatic to nonadiabatic behavior occurs at approximately 5.5 Å for the Fe case and 6.5 Å for the Mn case (Figure 3a). The face-to-face orientation is predicted to yield nonadiabatic behavior over the whole r range considered (Figure 3b). The face-to-face orientation also leads to similar $\kappa(r)$ behavior for the Fe and Mn cases. This contrasts the corner-to-corner orientation which displays significant differences in $\kappa(r)$ between Fe and Mn, and Fe $A_g(d_{xy})$ and Fe $B_g(d_{xz},d_{yz})$. These results demonstrate that the transmission probability is rather sensitive to the encounter orientation and it can be dependent on the electronic state of the reactants (i.e., the corner-to-corner Fe case in Figure 3a). This behavior derives primarily from the orientation and electronic structure dependence of the electronic coupling term V_{AB}.

Conclusions

Ab initio calculations have provided some new insights, as well as confirmation of some previous findings regarding the $Fe(OH_2)_6^{II/III}$ and $Mn(OH_2)_6^{II/III}$ self-exchange ET reactions. The internal reorganization energy depends strongly on the nature of the ET orbital, as expected. Thus, λ_I for the Mn case is substantially larger than for the Fe case. For the Fe case, we find a moderate effect on V_{AB}, depending on whether the minority spin electron occupies the d_{xy} orbital or a mixture of d_{xz}/d_{yz} in the Fe^{II} ion. While these two possible nearly isoenergetic electron-accepting states alter the magnitude and distance dependence of V_{AB}, they do not affect λ_I significantly.

The magnitude and distance dependence of V_{AB} are found to be strongly dependent on encounter orientation, as shown for the Fe case previously by Newton and co-workers. V_{AB} for the corner-to-corner encounter orientation is substantially larger at any given distance considered than that for the face-to-face encounter orientation. For the corner-to-corner encounter orientation, significant differences between Fe and Mn cases are apparent, while for the face-to-face encounter orientation, the magnitude and distance dependence of V_{AB} are rather similar. Values of the decay parameter β are in good agreement with well-accepted values. Adiabatic behavior ($\kappa \approx 1$) is predicted for the corner-to-corner encounter orientation at the shorter end of the ET distance range of 5−9 Å, while the face-to-face orientation is predicted to yield nonadiabatic behavior ($\kappa < 1$) over the entire range. The effects noted above in large part derive from the orientation and electronic structure dependence of V_{AB}.

Acknowledgment. This work was made possible by a grant from the U.S. Department of Energy, Office of Basic Energy Sciences, Geosciences Division. This research was performed in part using the Molecular Science Computing Facility (MSCF) in the William R. Wiley Environmental Molecular Sciences Laboratory at the Pacific Northwest National Laboratory. The MSCF is funded by the Office of Biological and Environmental Research in the U.S. Department of Energy. This work was supported in part by the Office of Advanced Scientific Computing Research, Office of Science, Department of Energy. Pacific

Northwest National Laboratory is operated by Battelle for the U.S. Department of Energy under Contract DE-AC06-76RLO 1830.

References and Notes

(1) Marcus, R. A.; Sutin, N. *Biochim. Biophys. Acta* **1985**, *811*, 265−322.

(2) Newton, M. D.; Sutin, N. *Annu. Rev. Phys. Chem.* **1984**, *35*, 437−480.

(3) Creutz, C.; Sutin, N. General reactivity patterns in electron transfer. In *Electron-transfer and electochemical reactions; Photochemical and other energized reactions*; Zuckermann, J. J., Ed.; VCH: Deerfield Beach, FL, 1986; Vol. 15, pp 47−68.

(4) Logan, J.; Newton, M. D. *J. Chem. Phys.* **1983**, *78*, 4086−4091.

(5) Newton, M. D. *J. Phys. Chem.* **1986**, *90*, 3734−3739.

(6) Newton, M. D. *J. Phys. Chem.* **1988**, *92*, 3049−3056.

(7) Rustad, J. R.; Rosso, K. M.; Felmy, A. R. *J. Chem. Phys.* **2004**, *120*, 7607−7615.

(8) Tembe, B. L.; Friedman, H. L.; Newton, M. D. *J. Chem. Phys.* **1982**, *76*, 1490−1507.

(9) Silverman, J.; Dodson, R. W. *J. Phys. Chem.* **1952**, *56*, 846−852.

(10) Jolley, W. H.; Stranks, D. R.; Swaddle, T. W. *Inorg. Chem.* **1990**, *29*, 1948−1951.

(11) Curtiss, L. A.; Halley, J. W.; Hautman, J.; Hung, N. C.; Nagy, Z.; Rhee, Y. J.; Yonco, R. M. *J. Electrochem. Soc.* **1991**, *138*, 2032−2041.

(12) Brunschwig, B. S.; Logan, J.; Newton, M. D.; Sutin, N. *J. Am. Chem. Soc.* **1980**, *102*, 5798−5809.

(13) Macartney, D. H.; Sutin, N. *Inorg. Chem.* **1985**, *24*, 3403−3409.

(14) Diebler, H.; Sutin, N. *J. Phys. Chem.* **1964**, *68*, 174−180.

(15) Franck, J. *Trans. Faraday Soc.* **1925**, *21*, 536.

(16) Condon, E. U. *Phys. Rev.* **1928**, *32*, 858.

(17) Marcus, R. A. *J. Chem. Phys.* **1956**, *24*, 966−978.

(18) Rosso, K. M.; Smith, D. M. A.; Dupuis, M. *J. Chem. Phys.* **2003**, *118*, 6455−6466.

(19) Landau, L. *Phys. Z. Sowjet.* **1932**, *1*, 89.

(20) Landau, L. *Phys. Z. Sowjet.* **1932**, *2*, 46.

(21) Zener, C. *Proc. R. Soc.* **1932**, *A137*, 696.

(22) Marcus, R. A. *Annu. Rev. Phys. Chem.* **1964**, *15*, 155−196.

(23) Apra, E.; Bylaska, E. J.; de Jong, W.; Hackler, M. T.; Hirata, S.; Pollack, L.; Smith, D. M. A.; Straatsma, T. P.; Windus, T. L.; Harrison, R. J.; Nieplocha, J.; Tipparaju, V.; Kumar, M.; Brown, E.; Cisneros, G.; Dupuis, M.; Fann, G. I.; Fruchtl, H.; Garza, J.; Hirao, K.; Kendall, R.; Nichols, J. A.; Tsemekhman, K.; Valiev, M.; Wolinski, K.; Anchell, J.; Bernholdt, D.; Borowski, P.; Clark, T.; Clerc, D.; Dachsel, H.; Deegan, M.; Dyall, K.; Elwood, D.; Glendening, E.; Gutowski, M.; Hess, A.; Jaffe, J.; Johnson, B.; Ju, J.; Kobayashi, H.; Kutteh, R.; Lin, Z.; Littlefield, R.; Long, X.; Meng, B.; Nakajima, T.; Niu, S.; Rosing, M.; Sandrone, G.; Stave, M.; Taylor, H.; Thomas, G.; van Lenthe, J.; Wong, A.; Zhang, Z. *NWChem: A computational chemistry package designed to run on high-performance parallel supercomputers*, version 4.5; Pacific Northwest National Laboratory: Richland, WA, 2003.

(24) Becke, A. D. *J. Chem. Phys.* **1993**, *98*, 1372−1377.

(25) Lee, C. T.; Yang, W. T.; Parr, R. G. *Phys. Rev. B* **1988**, *37*, 785−789.

(26) Rosso, K. M.; Rustad, J. R. *J. Phys. Chem. A* **2000**, *104*, 6718−6725.

(27) Ricca, A.; Bauschlicher, C. W. *J. Phys. Chem.* **1994**, *98*, 12899−12903.

(28) Russo, T. V.; Martin, R. L.; Hay, P. J. *J. Chem. Phys.* **1995**, *102*, 8023−8028.

(29) Martin, R. L.; Hay, P. J.; Pratt, L. R. *J. Phys. Chem. A* **1998**, *102*, 3565−3573.

(30) Rustad, J. R.; Dixon, D. A.; Rosso, K. M.; Felmy, A. R. *J. Am. Chem. Soc.* **1999**, *121*, 3234−3235.

(31) Rosso, K. M.; Morgan, J. J. *Geochim. Cosmochim. Acta* **2002**, *66*, 4223−4233.

(32) Schafer, A.; Huber, C.; Ahlrichs, R. *J. Chem. Phys.* **1994**, *100*, 5829−5835.

(33) Wachters, A. J. H. *J. Chem. Phys.* **1970**, *52*, 1033.

(34) Hay, P. J. *J. Chem. Phys.* **1977**, *66*, 4377.

(35) Clark, T.; Chandrasekhar, J.; Spitznagel, G. W.; Schleyer, P. V. *J. Comput. Chem.* **1983**, *4*, 294−301.

(36) Farazdel, A.; Dupuis, M.; Clementi, E.; Aviram, A. *J. Am. Chem. Soc.* **1990**, *112*, 4206−4214.

(37) King, H. F.; Stanton, R. E.; Kim, H.; Wyatt, R. E.; Parr, R. G. *J. Chem. Phys.* **1967**, *47*, 1936−1941.

(38) Frisch, M. J.; Trucks, G. W.; Schlegel, H. B.; Scuseria, G. E.; Robb, M. A.; Cheeseman, J. R.; Zakrzewski, V. G.; Montgomery, J. A., Jr.; Stratmann, R. E.; Burant, J. C.; Dapprich, S.; Millam, J. M.; Daniels, A. D.; Kudin, K. N.; Strain, M. C.; Farkas, O.; Tomasi, J.; Barone, V.; Cossi, M.; Cammi, R.; Mennucci, B.; Pomelli, C.; Adamo, C.; Clifford, S.; Ochterski, J.; Petersson, G. A.; Ayala, P. Y.; Cui, Q.; Morokuma, K.; Malick, D. K.; Rabuck, A. D.; Raghavachari, K.; Foresman, J. B.; Cioslowski, J.; Ortiz, J. V.; Stefanov, B. B.; Liu, G.; Liashenko, A.; Piskorz, P.; Komaromi, I.; Gomperts, R.; Martin, R. L.; Fox, D. J.; Keith, T.; Al-Laham, M. A.; Peng, C. Y.; Nanayakkara, A.; Gonzalez, C.; Challacombe, M.; Gill, P. M. W.; Johnson, B. G.; Chen, W.; Wong, M. W.; Andres, J. L.; Head-Gordon, M.; Replogle, E. S.; Pople, J. A. *Gaussian 98*, revision A.4; Gaussian, Inc.: Pittsburgh, PA, 1998.

(39) Nelsen, S. F.; Blackstock, S. C.; Kim, Y. *J. Am. Chem. Soc.* **1987**, *109*, 677−682.

(40) Klimkans, A.; Larsson, S. *Chem. Phys.* **1994**, *189*, 25−31.

(41) Eggleston, C. M.; Stack, A. G.; Rosso, K. M.; Higgins, S. R.; Bice, A. M.; Boese, S. W.; Pribyl, R. D.; Nichols, J. J. *Geochim. Cosmochim. Acta* **2003**, *67*, 985−1000.

(42) Zhang, X. D.; Wang, Y. N.; Guo, J. X.; Zhang, Q. Y. *J. Photochem. Photobiol., A* **1999**, *121*, 1−6.

(43) Weaver, M. J.; Yee, E. L. *Inorg. Chem.* **1980**, *19*, 1936−1945.

(44) Rosso, K. M.; Rustad, J. R.; Gibbs, G. V. *J. Phys. Chem. A* **2002**, *106*, 8133−8138.

(45) Sham, T. K.; Hastings, J. B.; Perlman, M. L. *J. Am. Chem. Soc.* **1980**, *102*, 5904−5906.

(46) Hamprecht, F. A.; Cohen, A. J.; Tozer, D. J.; Handy, N. C. *J. Chem. Phys.* **1998**, *109*, 6264−6271.

(47) Baker, J.; Pulay, P. *J. Comput. Chem.* **2003**, *24*, 1184−1191.

(48) Newton, M. D. *Coord. Chem. Rev.* **2003**, *238*, 167−185.

(49) Bu, Y.; Wang, Y.; Xu, F.; Deng, C. *THEOCHEM* **1998**, *453*, 43−48.

(50) Kanno, H. *J. Phys. Chem.* **1988**, *92*, 4232−4236.

(51) Johnson, D. A.; Nelson, P. G. *Inorg. Chem.* **1999**, *38*, 4949−4955.